Soft Matter

Influence of a nanoparticle on the structure and dynamics of model ionomer melts

Journal:	*Soft Matter*
Manuscript ID	SM-ART-03-2018-000665.R1
Article Type:	Paper
Date Submitted by the Author:	10-May-2018
Complete List of Authors:	Sampath, Janani; Ohio State University, Chemical and Biomolecular Engineering Hall, Lisa; The Ohio State University,

Influence of a Nanoparticle on the Structure and Dynamics of Model Ionomer Melts

Janani Sampath and Lisa M. Hall*

William G. Lowrie Department of Chemical and Biomolecular Engineering, The Ohio State University, 151 W. Woodruff Ave., Columbus, OH 43210

*E-mail: hall.1004@osu.edu

We simulate a single spherical nanoparticle (NP) surrounded by partially neutralized ionomers. The coarse-grained ionomers consist of a linear backbone of neutral monomer beads with charged pendant beads and counterions, along with pendant 'sticker' beads that represent unneutralized acid groups. Two different NP interactions are considered; one in which the NP interacts uniformly with all beads in the system (neutral NP) and another in which the NP has higher cohesive interactions with ions and stickers (sticky NP). Ions are depleted around the neutral NP relative to the bulk, but are denser around the surface of the sticky NP. The bond vector autocorrelation function was computed as a function of distance from the NP. For the neutral NP, due to the absence of ions, there is an increase in bond rotational dynamics near the surface relative to the bulk, while the reverse trend is observed in the case of the sticky NP. These analyses were done systematically for differing mole content of pendants, levels of neutralization, and NP sizes; lower pendant content causes a significantly larger difference in the bond dynamics near and far from the NP surface.

Introduction:

Polymer nanocomposites (PNCs) have been at the forefront of engineering research for the past several decades, with broad applications ranging from aviation to drug delivery.[1,2] Incorporating a small fraction of NPs into a polymer matrix can bring about a large enhancement of the materials the mechanical, electrical, or optical properties, versus the pure polymer due to a dynamic coupling between polymer chains and NPs.[3,4] Therefore, rigorous understanding of microscopic effects is needed to enhance the performance and subsequent application of PNCs. In light of this, experimental[5,6] as well as theoretical studies[7,8] have been undertaken, establishing that polymers behave differently when confined near an interface or near a filler surface compared to the bulk.[9,10] While most of this fundamental work on polymer-filler interactions and interfacial behavior has focused on homopolymer PNCs, here we consider NPs incorporated into ionomers, polymers which contain a small fraction of ionic groups (up to 15%).[11] Ionomers are of interest for use with NPs due to their favorable mechanical properties and potential for specific interactions with the NP surface; for instance, ionomers can increase the dispersion/exfoliation of certain silica or clay NPs.[12,13]

General ionomer behavior is relatively well understood; it is clear that by introducing ions into a polymer with a low dielectric constant, large enhancements in the material's mechanical and transport properties are brought about due to the formation of nanoscale ionic aggregates.[14–16] Here, we consider poly(ethylene-co-methacrylic acid) (PEMAA) partially neutralized by sodium, similar to the commercially available material Surlyn®, but without any branching (our chains have a linear backbone).[17] A closely related material, partially neutralized poly(ethylene-co-acrylic acid) (PEAA), has been

extensively studied in the past through both experiments[14,18–20] and simulations.[21–31] Often, aggregate ordering was quantified by studying the characteristic peak at low wavevectors in X-ray scattering, known as the ionomer peak.[32,33] Overall, the morphology of the aggregates in these systems and how this depends on controllable features of ionomers such as concentration of ionic groups has been well described.

We use coarse-grained molecular dynamics simulations to understand the structure and dynamics of such a partially neutralized ionomer as a function of distance from a hard NP, with a particular focus on how ionic aggregates are impacted by the NP. This work builds upon prior experimental as well as simulation efforts that have studied the behavior of associating polymers near a flat surface,[34–36] as we expect ionic groups may behave similarly near the interface of a spherical NP. This expectation is based on prior work on homopolymer systems that made analogies between polymer behavior near a flat surface and near a NP interface. For instance, Bansal et al., while studying polysulfone interfaces with NPs, showed that the behavior of polymers in PNCs is quantitatively similar to that in planar polymer films, specifically by comparing the change in T_g with film thickness and NP loading.[37] The simulation study of Starr et al. also suggested a similarity in the morphology of polymers close to the surface in ultrathin films and near NP fillers, with polymers being elongated and flattened at either type of interface.[38]

Both simulation[34,35] and experimental[36] work on self-associating polymer films has shown that there is a strong depletion of functionalized or associating groups at the interface. In particular, for thin PEAA ionomer films, AFM indicates that ethylene groups populate the surface, with the ionic aggregates present a few nanometers below the surface.[36] Ayyagari et al. suggested that this inhomogeneity is due to the ionic aggregates

or clusters preferring to have configurations similar to those in the bulk (as opposed to flattening out near the interface).[35] Relatedly, Simmons and coworkers' simulation study made analogies between the glassy behavior of homopolymers near a NP and the behavior of the backbone segments of ionomers near the ionic aggregates.[39,40]

None of the prior ionomer simulation work described above included NPs. However, we can adopt a model for the NP similar to one of those used in the multiple prior coarse-grained MD simulations of PNC systems, though these were typically used with homopolymers. In particular, NPs have been represented in coarse-grained polymer simulations in several different ways, with different NP-monomer interactions.[7,8,41–48] The most straightforward in terms of setting the interactions is to explicitly represent NPs as a collection of monomer-sized beads (that each interact with monomers with the same potential form used for monomer-monomer interactions) that are rigidly joined together; Smith et al. considered such large, roughly spherical NPs[42], while Starr et al. considered icosahedral particles.[7,41] However, representing a NP as a single perfectly smooth sphere (as one particle in the simulation) is less computationally intensive. Some have considered single-site NPs and simply set the same LJ potential form for NP-monomer interactions as for monomer interactions,[43,44] but for large NPs this would lead to a much wider well depth for the NP-monomer than monomer-monomer interactions, leading to a particle surface that is essentially softer than a wall of monomers would be.

One way to account for the discrepancy in size between the monomer beads and NP while keeping the NP-monomer and monomer-monomer interactions more locally similar is to use a radially shifted LJ potential.[45,46] In this case, setting NP-monomer and monomer-monomer interaction strengths equal would mean that the particles are

effectively repulsive, because monomers that contact the large NP cannot contact as many monomers (they gain only one unit of the monomer-monomer interaction strength through the NP interaction, but would be able to participate in multiple additional interactions with other monomers if they were in the bulk). A more straightforward way to consider a NP that is composed of units that are chemically similar to monomers is to use a "colloid" potential, which is derived by integrating over the LJ interaction between one monomer bead with a spherical NP composed of a continuum of other LJ beads at uniform density. in't Veld et al. found this potential to more accurately describe the liquid-vapor coexistence of pure NP systems compared to the shifted LJ potential.[47] Kalathi et al. also employed this potential to study chain relaxation in homopolymer PNCs as a function of NP size and chain length.[8] In the current work, we use such a colloid potential and consider two sets of interaction strengths with monomers as described below.

In this work, we introduce a single NP in our simulation box, eliminating the need to equilibrate the positions of many NPs interacting in a polymer matrix, which would be intractable. The effect of NP volume fraction is relatively well known, with an increase in NP volume fraction leading to a decrease in the overall dynamics of polymers because polymer motion is constrained near the NP surface and as volume fraction increases more polymers are impacted.[49–51] By simulating with just one NP, we can focus on the interfacial effects alone, and the polymers can effectively equilibrate around the NP as long as the simulation extends many times the polymer relaxation time. Previous homopolymer PNC work has established that adding NPs leads to dynamic heterogeneity near and far from the interface, with the polymer mobility decreasing close to an

attractive NP surface as compared to the bulk (or increasing for a neutral NP).[52] We also consider different NP-monomer interaction strengths because for homopolymers, it is known that the drastic improvements in viscoelastic and mechanical properties upon NP addition are due to changes in polymer relaxation around NPs, which is dependent on the NP-polymer interactions.[42,51] Generally, an attractive polymer-NP interaction increases the local relaxation time and viscosity of the system, while the reverse is true for an unfavorable polymer-NP interaction (which may also lead to NP aggregation and reduction of the effects of the NPs on the polymer). Overall, we aim to understand the important effects present in bulk PNC systems by probing the change in bond rotational dynamics of the ionomer near the single NP surface vs. the bulk in for both neutral and attractive NPs. We also describe how far from the surface the effect of NP persists.

Model:

We consider a dense melt of PEMAA ionomers partially neutralized with sodium, with anions randomly placed pendant to the uncharged backbone and an equal amount of unbound counterions added to make the system neutral. We use a simple coarse-grained model with the model parameters detailed in reference 17, and review the model briefly here.

All monomers are modeled according to the bead spring model of Kremer and Grest.[53] Bonded beads interact via the finitely extensible non-linear elastic (FENE) potential, given by:

$$U_{FENE}(r) = \begin{cases} -0.5kR_0{}^2 ln\left[1 - \left(\frac{r}{R_0}\right)^2\right], & r < R_0 \\ \infty, & r \geq R_0 \end{cases}$$

where R_0 is the maximum extent of the bond, set to 1.5σ, and $k = 30\varepsilon/\sigma^2$ is the spring constant, making the spring short and stiff to avoid chain crossing.[53] σ and ε are the reduced units of length and energy, respectively.

All beads interact via the truncated and shifted Lennard-Jones (LJ) potential given by:

$$U_{LJ,ij}(r) = \begin{cases} 4\varepsilon_{ij}\left[\left(\frac{\sigma_{ij}}{r}\right)^{12} - \left(\frac{\sigma_{ij}}{r}\right)^{6} + S\right], & r < r_c \\ 0, & r \geq r_c \end{cases}$$

where the shift factor S makes the potential 0 at the cutoff, r_c. All monomers have LJ diameter σ = 1.0, and ε = 1.0 for backbone monomer interactions. For bonded beads, $r_c = 2^{1/6}\sigma$ while for non bonded beads, we have included the attractive tail of the potential to a distance of $r_c = 2.5\sigma$. Our mapping to PEMAA is as shown in Figure 1; three methyl groups (including the one attached to the uncharged bead to which the pendant group is also attached) along the backbone map to one monomer bead, which is modeled as the same size as the sticker or anion groups pendant to the backbone that represent either COOH or COO^-, respectively. These monomer beads are twice the size of the unbound counterion beads. Due to the approximate size of these groups and the ionic radius of Na^+, we map the monomer diameter σ to 0.4nm in real units (and the counterion diameter

to 0.2nm).[25] All beads have unit mass. ε_{ij} = 1.0 is the interaction strength between all beads except for sticker-sticker and sticker-ion interactions. The sticker groups were added to mimic hydrogen-bonding groups and have an increased short ranged interaction with other stickers or ions (though unlike hydrogen bonds, the interactions are radially symmetric). We keep the current model similar to the prior ionomer model of Hall et al.,[25,26] modifying only the sticker-sticker and sticker-ion LJ interaction strengths to account for the associating nature of the sticker groups. The sticker-sticker, sticker-anion, and sticker-counterion LJ interaction strengths are ε_{ss}= 2.0, ε_{sa}= 1.5, and ε_{sc}= 4.5, respectively, which yield local aggregate structures comparable to atomistic simulations of a similar material; details can be found in reference 17. We were also able to reproduce the overall experimental rheological trends of PEMAA with different acid contents and an esterified analog using this model.[15,16] All systems have chain lengths of 36, below the entanglement length for Kremer Grest polymers.[53]

The counterions and anionic pendant groups interact via the long ranged Coulombic potential:

$$U_c(r) = \frac{q_1 q_2}{4\pi\varepsilon_o\varepsilon_r r}$$

where ε_o is the vacuum permittivity, ε_r is the background dielectric constant accounting for the chemistry of the uncharged backbone which reduces the Coulombic interaction between ions (as partial charges or polarizability are not included in our coarse-grained model), and q_1 and q_2 are the charges of +1e or -1e. Based on prior work[17,25] we choose ε_r

= 4, setting the dielectric constant in reduced units to 0.028. This implies that the interaction between two unit charges at a distance of 1.0σ is (1/0.028)ε.

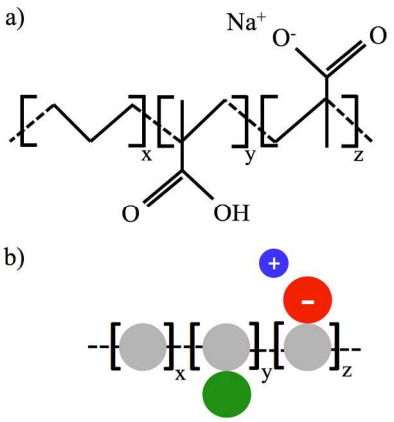

Figure 1: (a) Chemical structure of the ionomer modeled in this study (PEMAA) with pendant groups placed randomly along the chain, and (b) coarse-grained representation of the system with the anion shown in red, counterion in blue, sticker in green, and neutral monomers in gray, as in the snapshots below.

As shown in Figure 1, pendant groups can be stickers (COOH) or anions (COO^-) and are placed randomly along the backbone. We report total pendant group concentration as the number of backbone beads (N_{bb}) per pendant bead, setting this to 3, 5, or 7 to allow comparison to prior work. We also vary the level of neutralization (defined as the percentage of anions to total pendants; a higher neutralization means higher ion density). For a given neutralization level, N_{bb} = 7 has the lowest ion density. The PEMAA modeled is similar to the commercial ionomer Surlyn, although Surlyn would have longer chains with some branching, while we consider only unentangled, linear chains. We name our systems in a format of "N_{bb}#-%Na"; for example, N_{bb}5-50%Na has an average backbone spacing of 5 between pendant groups and 50% of its pendant groups are charged. We consider four levels of neutralization: 10, 25, 50 and 75%.

We represent the NP as a smooth particle of diameter 10σ for most of this work. We also consider NP diameters of 12.5σ and 7.5σ for N_{bb}5-50%Na systems while maintaining a constant NP volume fraction of 1.1%. Accordingly, systems with NP sizes of 12.5σ, 10σ, and 7.5σ have a total of 1600, 800, and 400 polymers, respectively (800 polymers are used for all 10σ NP systems even though the different numbers of pendant groups at N_{bb} = 3 and N_{bb} = 7 means that these have slightly different NP volume fractions). The average polymer radius of gyration is 3.5σ for the systems considered here, implying that the NP size relative to the characteristic chain size is 1.1, 1.4, and 1.8 for NP sizes of 7.5σ, 10σ, and 12.5σ, respectively. Although the size of our polymers are small in comparison to the NP diameters considered,[8,54,55] there are multiple length scales of interest in ionomers; particularly, the local and long range ionic aggregate structure. The range of NP sizes considered enable us to study whether NP curvature (albeit within a small range) significantly impacts such structures." The NP interacts with beads via the "colloid" potential, derived by considering the total interaction of an LJ particle with a spherical NP composed of smaller LJ particles at uniform density ρ_{NP} ("smeared out" evenly throughout the sphere). Specifically, the interaction between a NP and a monomer or counterion bead (all denoted by the subscript B below) can be obtained by analytically integrating over all LJ particles within the NP sphere and is given by:[8,47,48]

$$U_{NP-P}(r) = \frac{2R_{NP}^3\sigma_{NP-B}^3 A_{NP-B}}{9(R_{NP}^2 - r^2)^3} \times \left[1 - \frac{(5R_{NP}^6 + 45R_{NP}^4 r^2 + 63R_{NP}^2 r^4 + 15r^6)\sigma_{NP-B}^6}{15(R_{NP} - r)^6(R_{NP} + r)^6}\right]$$

for $r < r_c$, where R_{NP} is the radius of the NP and we use $\sigma_{NP-B} = 1.0$. The Hamaker constant for NP-solvent interaction is given by $A_{NP} = 24\pi\varepsilon_{NP}\rho_{NP}\sigma^3$. We consider the NP is composed of LJ particles the size of a monomer bead (1σ) and with density $\rho_{NP}\sigma^3$

= 0.89 (similar to the density of an attractive Kremer-Grest melt). In order to test the effect of NP interaction parameter, we simulated systems with two sets of NP-sticker and NP-ion interactions (NP-backbone interaction is the same for both). For the first set of interaction parameters, we consider a neutral NP effectively composed of backbone beads; all NP-bead interactions are the same with $\varepsilon_{NP-B} = \varepsilon = 1.0$ ($A_{NP-B} = 67.1$). For the second set of interaction parameters, the NP was treated as if it were composed of stickers, with an interaction strength of $\varepsilon_{NP-N} = 1.0$ ($A_{NP-N} = 67.1$) with neutral monomers, $\varepsilon_{NP-S} = 2.0$ ($A_{NP-S} = 134.2$) with stickers, $\varepsilon_{NP-A} = 1.5$ ($A_{NP-A} = 100.7$) with anions, and $\varepsilon_{NP-C} = 4.5$ ($A_{NP-C} = 302$) with counterions. The NP is referred to as 'neutral' for the first case or 'sticky' for the second. The cutoff $r_c = \frac{\sigma_{NP}}{2} + 4\sigma$, and depends on the NP diameter. Note that the effective NP diameter is larger than σ_{NP}; this is because the NP is an amalgamation of spheres of size 1σ whose centers can exist at the surface of the sphere. See Supporting Information for plots including a comparison between our NP-bead potentials and radially shifted LJ potentials. The NP was kept fixed at the center of the box. As mentioned above, the particle volume fraction is low, at approximately 1%. We computed average properties (end to end relaxation and mean square displacement, see Supporting Information for more details) for all monomers in the NP-containing system, and found very little difference in these properties for the NP-containing system versus the analogous pure ionomer system, as expected for such a low loading fraction.[8,51] Bulk properties of the systems considered here (without a NP) can be found in prior work.[17] In the following, we focus on the impact of the NP on the polymer 2-4σ from the interface.

Our NP-bead interaction parameters are similar to those used in prior work. In particular, Smith et al.[42] investigated homopolymer PNCs with neutral ($\varepsilon_{NP-B} = 1.0$) and attractive ($\varepsilon_{NP-B} = 2.0$) NP-polymer interactions where the NP was composed of monomer-sized LJ beads. Relatedly, in order to study the effect of hydrogen bonding on homopolymer nanocomposites, Liu et al. simulated a system with $\varepsilon_{NP-B} = 10.0$, where the NP-monomer interaction was a radially shifted LJ potential.[45] In these homopolymers studies, all monomer-NP interactions were the same, however, we include different sticker-NP, ion-NP, and backbone-NP interactions for our attractive system to account for the chemical differences of our coarse-grained beads.

All simulations were carried out using LAMMPS molecular dynamics package.[56,57] To initialize the simulation, chains are placed as random walks and counterions are placed randomly in the box; a soft pairwise potential is briefly applied to push overlapping beads off of each other before turning on the pairwise LJ interactions. We first run a simulation in the NPT ensemble using a Nose-Hoover thermostat and barostat, setting pressure to 0 with a pressure damping parameter 100τ. The systems are simulated in NPT for 10,000τ to determine the appropriate density. Specifically, we calculate the average box size after excluding the first 5% of the run (before the density was approximately constant) and use this as our box size for the subsequent constant volume run. We then equilibrate the system in the NVT ensemble for $2\times10^5\tau$ (using the same thermostat and no barostat). During this time, the mean squared displacement for the polymers was greater than $3R_g^2$. After equilibration, data was collected during another NVT run of $10^5\tau$. In both the initial NPT and both NVT runs, the temperature damping parameter of 1.0τ was used to maintain the temperature at T* = 1.25 where reduced temperature T* = 1.0kT/ε. More

details on this temperature choice can be found in Ref 28; briefly, we employ this increased temperature as it allows the system to equilibrate in a reasonable simulation time as we include the attractive portion of the LJ potential which slows down the dynamics compared to the fully repulsive model used in prior work.[25] We use periodic boundary conditions and a velocity-Verlet algorithm with a time step of 0.005τ.

Results:

We first present images to qualitatively show the distribution of monomers around the NP; all images are produced using the MD visualization software VMD.[58] Figure 2 shows three systems with different average pendant spacing at the same neutralization (50%Na), with the top and bottom rows for the neutral and sticky NPs, respectively. From the top row, Figures 2(a-c), it can be seen that the ions are depleted near the neutral NP interface, for about 2 monomer diameters from the NP for all three spacer lengths. This effect is as expected based on the depletion of ions near flat surfaces,[35,36] as aggregates further from the NP can maintain the same size and shape as in the bulk and better preserve their long-range order.

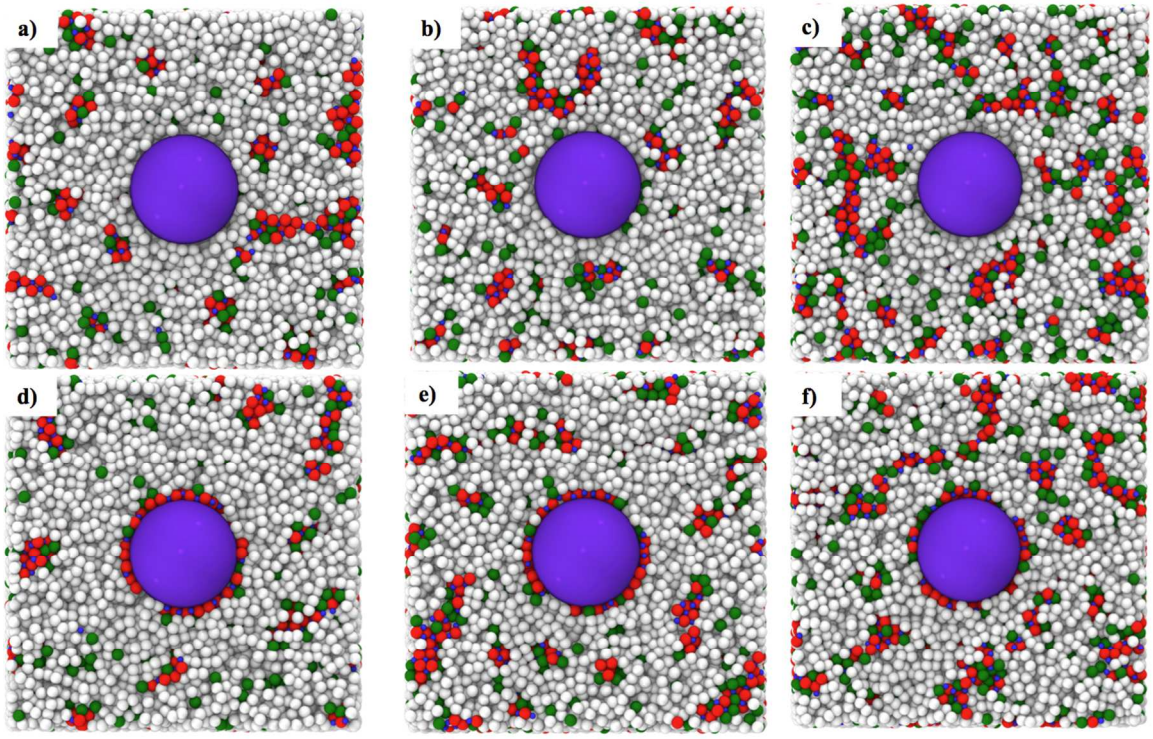

Figure 2: Snapshots showing NP in purple, backbone in white, stickers in green, anions in red, and counterions in blue for three systems at 50% neutralization with average spacer length of N_{bb} = 7 (a,d), N_{bb} = 5 (b,e), N_{bb} = 3 (c,f); a-c (top row) are for a neutral NP and d-f (bottom row) are for a sticky NP.

When the NP has sticker-like interactions, Figures 2(d-f), all systems are able to form a relatively dense layer of ions around the sticky NP.

The second set of systems we considered has a constant average pendant spacing of N_{bb} = 3 and a variety of neutralization levels. Snapshots of this set of systems are presented in Figure 3, where going from left to right there is a decrease in the number of stickers (green beads) and increase in the number of ions (red and blue beads) as the neutralization increases from 10% (Figures 3(a,e)) to 75%(Figures 3(d,h)). Note that the third system of this set, N_{bb}3-50%Na, is repeated from above to more clearly present the effect of increasing neutralization (Figure 2c and f are the same as Figure 3c and g, and this repetition also occurs in the later figures). The relative distribution of different

groups around the NP is similar to that observed in Figure 2. Ions are depleted around the neutral NP (Figures 3(a-d)) but are densely ordered around the sticky NP (Figures 3(e-h)), with the number of ions around the NP increasing with an increase in neutralization.

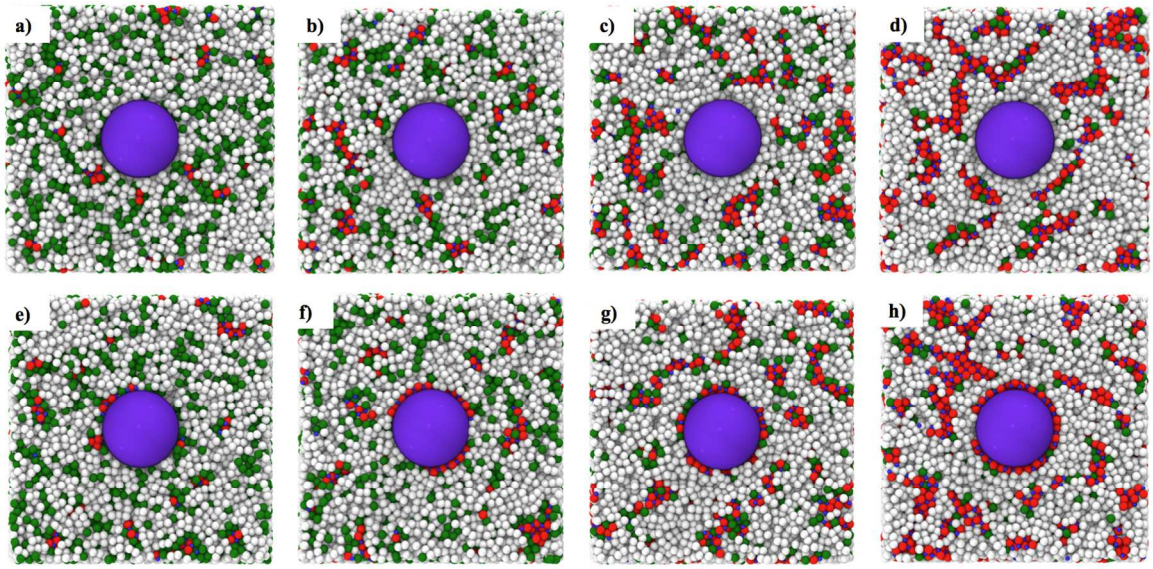

Figure 3: Snapshots showing NP in purple, backbone in white, stickers in green, anions in red, and counterions in blue for systems with an average spacer length of N_{bb} = 3 at 10%(a,e), 25% (b,f), 50% (c,g), and 75% (d,h) neutralization; a-d (top row) are for a neutral NP and e-h (bottom row) are for a sticky NP.

We quantitatively assess the packing around the NP via the radial distribution functions $g_{ij}(r)$, the normalized probability of a bead of type i existing at a distance r from a bead of type j. We report $g_{ij}(r)$ in Figures 4 and 5 for the same systems discussed above, showing correlations of the NP with uncharged backbone beads, stickers, and ionic groups, where we include both NP-Counterion and NP-Anion correlations together in the NP-Ion g(r). For all systems, the first NP-Backbone and NP-Sticker peaks are sharp and followed by smaller σ-scale oscillations due to monomer-scale ordering at the relatively flat, smooth interface of the NP. Note that the NP diameter 10σ represents the core of the NP; the NP-

Backbone and NP-Sticker first peaks show the effective NP diameter is approximately 10.7σ; see the Supporting Information for a discussion of effective NP size when using the colloid potential vs. the radially shifted LJ potential. For all sticky NP systems (bottom rows of Figures 4 and 5), an NP-Ion peak exists at the same distance as the first NP-Backbone peak due to packing of ions on the NP surface. The Sticky NP-Sticker correlations show a strong second peak at about 0.8σ further, due to stickers packing near this first layer of ions. However, these surface peaks are absent in all neutral NP systems' NP-Ion correlations; as discussed above, ions are depleted near the neutral NP surface. Instead, the first neutral NP-Ion peak is several σ from the surface and is also relatively broader than the monomer scale ordering peaks, as it is due to the average packing of aggregates around the NPs. The sticky NP systems all show a similar broad NP-Ion peak away from the surface, though it is further from the surface than the neutral NP-Ion peak, likely because the ionic aggregates are ordering based on their preferred distance from the ions at the sticky NP surface. To further show the effect of a nanoparticle on the aggregate ordering, we also computed the Ion-Ion structure factor of three systems (N_{bb} = 3 at neutralizations of 25%, 50%, and 75%) with and without a nanoparticle; this is presented in the Supporting Information.

To explain the impact of ion content on aggregate ordering, we first discuss the N_{bb} = 7, 5, and 3 systems (reducing average spacing of pendants along the chain) at constant 50% neutralization; these systems' $g_{ij}(r)$ are given in Figure 4. Figures 4(a-c) are for the neutral NP systems, and the position of the first NP-Ion peak is at 8.55σ, 9.15σ, and 9.65σ for N_{bb}3-50%Na, N_{bb}5-50%Na, and N_{bb}7-50%Na, respectively, whereas the first NP-Backbone peak is at 5.85σ. As the ion density increases, the NP-Ion peak moves to

lower r and the peak becomes somewhat narrower, meaning the ionic aggregates are slightly more ordered and closer to the NP. The sticky NP-Ion correlations in Figures 4(d-f) show a strong first peak at the surface, with peak heights (not shown) of approximately 22, 18, and 14 for N_{bb}7-50%Na, N_{bb}5-50%Na, N_{bb}3-50%Na, respectively. The second sticky NP-Ion peak describing ionic aggregate packing around the NP behaves relatively similarly to the first neutral NP-Ion peak, in that it also shifts to shorter distance and sharpens as ion content increases.

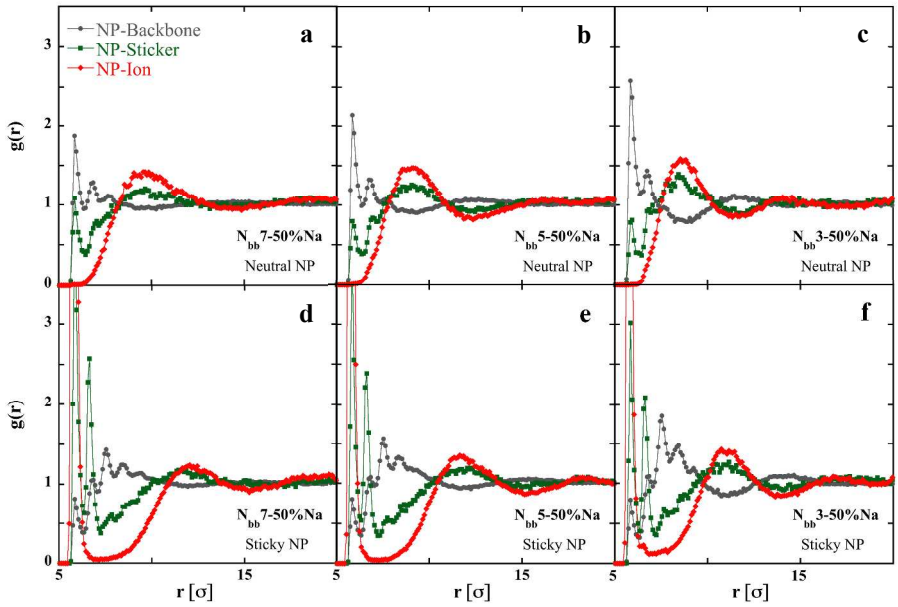

Figure 4: NP-Backbone, NP-Sticker, and NP-Ion pair correlation functions, as labeled, for three systems at 50% neutralization with average spacer length of N_{bb} = 7 (a,d), N_{bb} = 5 (b,e), N_{bb} = 3 (c,f); a-c (top row) are for a neutral NP and d-f (bottom row) are for a sticky NP.

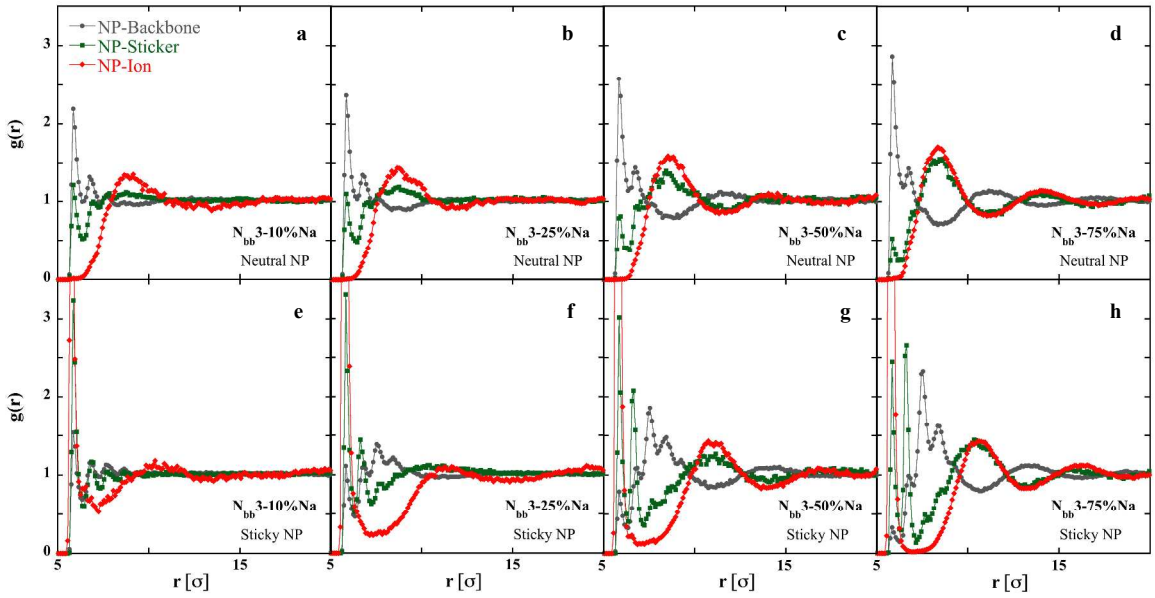

Figure 5: NP-Backbone, NP-Sticker, and NP-Ion pair correlation functions, as labeled, for systems with an average spacer length of N_{bb} = 3 at 10%(a,e), 25% (b,f), 50% (c,g), and 75% (d,h) neutralization; a-d (top row) are for a neutral NP and e-h (bottom row) are for a sticky NP.

We now consider the second set of systems to show the effect of increasing ion content by increasing neutralization at constant average pendant spacing; Figure 5 shows $g_{ij}(r)$ for these systems. As was the case for the 50% neutralized systems in Figure 4, the first NP-backbone peak occurs at 5.85σ. For the neutral NP systems Figures 5(a-d), the first NP-ion peaks represent aggregate ordering around the NP and occur at 8.65σ, 8.65σ, 8.55σ, and 8.35σ for neutralizations of 10%, 25%, 50% and 75% respectively (Figures 5(a-d)). As in Figure 3, we find that ions are more ordered and closer to the NP with increasing ion content. For the case of the sticky NP (Figures 5(e-h)), the first NP-Ion peak (showing packing at the NP surface) has a height of 5 for N_{bb}3-10%Na system, then approximately 14 for the three higher neutralization systems of 25%, 50% and 75%. Also, between the first and second peaks in the sticky NP-Ion g(r), the ion density goes to

zero only for the N_{bb}3-75%Na system. With fewer stickers, the ions tend to pack into relatively more discrete shells (similar to the trend observed for the systems at 50% neutralization with different spacer lengths from Figure 4).

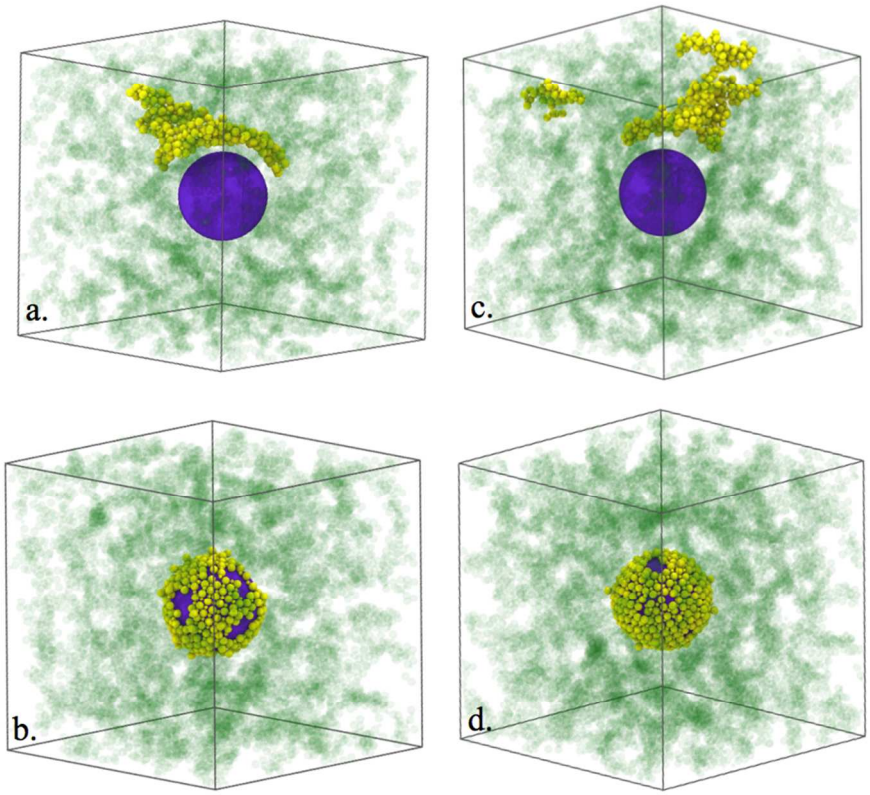

Figure 6: Snapshots of aggregate packing around a NP; all aggregates are translucent green except for the selected one near the NP, in yellow; (a,b) and (c,d) are for the N_{bb} = 3 system at 50% and 75% neutralization, respectively; the NP is neutral in (a,c) and sticky in (b,d).

The depletion of ions near the neutral NP surface can be likened to the depletion of functionalized or ionic groups near an interface of a freestanding film, which has been discussed in prior works. Specifically, Smith and coworkers report a strong depletion of associating 'sticker' groups in simulations of a functionalized polymer near a neutral free surface; this effect persists for a significant distance, introducing structure in associating

groups perpendicular to the interface[35]. Relatedly, using AFM, Sauer et al.[36] resolved ethylene rich lamella near the surface of PEMAA films.

In order to analyze how clusters order themselves around the NP, we performed a cluster analysis in the same manner as prior work.[17] Specifically, we consider any anion and cation within 0.79σ of each other to be part of the same cluster; a sticker is added to the same cluster as another sticker, anion, or cation if it is within 1.05σ of that bead. Only those clusters that have more than 2 counterions are included in later analysis (which includes over 94% of the counterions in the system), similar to the analysis of reference 17 in which we also report detailed cluster morphologies and cluster autocorrelation functions for the pure ionomer systems. For systems with low ion density (spacer lengths above N_{bb} = 3 and neutralizations below 50%), clusters appear similar in shape both near and far from the neutral NP, as they are mostly discrete and compact. However, for systems with higher ion content with long and branched aggregates, the aggregates appear to wrap around the neutral NP (conform to the spherical shape) while staying about 2-3σ away from the surface, as seen in Figures 6a and 6c for N_{bb}3-50%Na and N_{bb}3-75%Na, respectively. For the case of the sticky NP, it is seen from Figure 6(b,d) that the ions stick to the surface of the NP, forming a well ordered layer that is its own cluster. Clusters further from the sticky NP surface appear relatively similar to those in the bulk.

We expect the inhomogeneity in structure of the ionomer around the NP also leads to a change in dynamics near the NP. Prior work suggests that the impact of the NP on local dynamics will depend on the NP-monomer chemical interactions. Specifically, Smith et al.[42] reported that chain dynamics is slower when monomers are attracted to the NP,

compared to systems that have only repulsive interactions. Kalathi et al.[8] and Schneider et al.[59] have reported, through coarse-grained simulations and experiments, respectively, that weakly attractive NPs do not affect monomeric relaxation rates. All these results were for homopolymers below the entanglement limit.

To understand changes in local dynamics brought about by the NP in our systems, we compute bond autocorrelation function, BACF $= \langle \vec{B}_s(t) \cdot \vec{B}_s(0) \rangle$, where $\vec{B}_s(t)$ is bond vector at time t, and angle brackets represent averaging over all bonds in specific shells around the NP. It is normalized by the value at time 0. We consider distance from the nanoparticle in an approach similar to that of Ghanbari et al. (note that this work computes intermediate scattering function and not BACF).[52] Specifically, we consider concentric spherical shells of thickness 2σ around the NP (starting at a radius of 5.5σ), where a bond is assigned to the shell where its center was located at time $\tau = 0$ (note that we do not consider the residence time of the bond in that shell). Below, we discuss only the first shell near the NP versus the bulk results, as the material quickly returns to bulk behavior at longer distances (see the Supporting Information).

To provide context for the BACF, we recall the Rouse model that describes polymer chain dynamics in a melt; there are p Rouse modes for a polymer chain of length N, where p = 0,1,2,...,N-1. The largest mode (N-1) describes the relaxation of bond segments. Prior work reported that the relaxation times of different modes of polymers around a neutral nanoparticle follow the same scaling as in the bulk; thus, the deviation of one of the modes from the homopolymer value gives a good overall measure of the impact of the NP on surrounding polymer.[8,42,50] For an attractive NP, Smith et al. find that the influence of the NP is more pronounced for larger modes,[42] thus, the bonds show the

most difference. In this work, we consider bonds as a small and sensitive measure of changes due to NPs that allows us to accumulate good statistics over small volumes (shells close to NPs). Specifically, we consider the BACF, a measure of orientational relaxation of bonds (not translational relaxation). Similarly, prior work of Heffernan et al. has reported on the bond vector rotational relaxation times for simple Kremer-Grest chains.[60]

We report the BACF for systems at the same neutralization and different spacer lengths (Figure 7) and systems at the same spacer length for different neutralizations (Figure 8). For context, we also report BACF values for a neutral NP and homopolymer system (with no ions or stickers) with chain length N = 35 in the Supporting Information. For the homopolymer system, there is a slight increase in mobility near the NP surface, with the bonds in the first shell relaxing faster than those in the bulk. This effect is mainly due to the excluded volume created at the interface, where particles are not as tightly packed as they are in the bulk. In previous coarse-grained simulation work, Starr et al. observed this effect as well.[7,38]

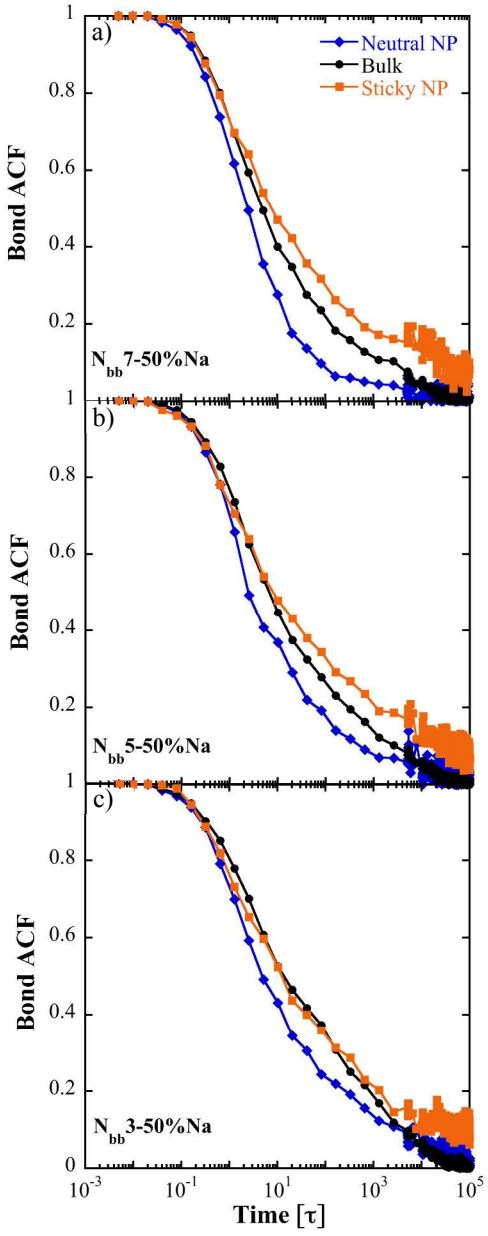

Figure 7: Bond vector autocorrelation function for bonds near the surface of a neutral or sticky NP or in bulk, as labeled, for (a) N_{bb} = 7, (b) N_{bb} = 5, and (c) N_{bb} = 3 systems at 50% neutralization.

From Figure 7, it can be seen that the bonds near the neutral NP relax faster than those in the bulk, while bonds near the sticky NP relax slower. It is known that the introduction of even a few ionic groups constrains the motion of the polymer chain, and the dynamics of

associating ion-containing polymers are much slower then that of their neutral counterparts.[17,28,61] Hence, the inhomogeneity in dynamics can be understood in terms of the distribution of ions around the NP. For the neutral NP, there are no ions present in the first shell around the NP, thereby increasing the relaxation of the interfacial bonds compared to the bulk. For the sticky NP, as there are excess ions at the interface compared to the bulk, bond relaxation is slowed. The separation in dynamics is most pronounced for the N_{bb}7-50%Na system, and becomes less pronounced as the spacer length decreases. Considering the overall change in relaxation as a function of average pendant spacing, we note that the polymers relax more quickly at higher spacings and this is in accordance with prior work. The bonds in the longer spacing systems are relatively less constrained, due to fewer ions beings present overall. Note that although the N_{bb}3-50%Na sticker NP relaxation closely follows the bulk, it does not completely relax (go to zero) at long times. This is because of the strong adsorption to the surface; about 15% of ions that were present near the interface at 0τ are at the surface at $10^5\tau$ (the time over which the BACF is calculated). However, considering the overall equilibration period of $2\times10^5\tau$, only 5% of the ions initially present on the surface are on the surface at the end of that time (only slightly higher than the overall percentage of ions that are adsorbed at any given time, 4%).

From Figure 8, it is seen that as the neutralization increases, there is a greater difference between the BACFs for the polymers in the bulk, near the neutral NP, and near the sticky NP. For the systems of N_{bb}3-10%Na and N_{bb}3-25%Na, there is almost no difference between the neutral and sticky NP interfaces, and both of these have relaxations very close to the bulk relaxation. This is due in part to the smaller number of ions, but also due

to the fact that the ions are more disperse due to the large number of stickers in these systems (Figure 5). For N_{bb}3-50%Na, the difference in dynamics becomes more apparent, and the bonds near the sticky NP interface do not fully decorrelate even at $10^5\tau$. However, this effect is most apparent for the N_{bb}3-75%Na system where the dynamics near the sticky NP interface is severely constrained due to the large number of ions around the NP. (27% of ions initially on the surface are on the surface at $10^5\tau$ for this system, compared to 6% of all ions adsorbed on the surface overall.) Interestingly, for the systems that have neutralization < 75%, the BACF near the sticky NP is somewhat faster at short times than the bulk, even though there are more ions near the sticky NP than in the bulk. We surmise that the stickers present with the ions serve to speed up short time dynamics. The facilitation of ion dynamics by stickers has been reported in prior work.[17]

Here, we study only a very low loading fraction and focused on interfacial effects. However, it is clear that, in systems where NPs are added to ionomers to change the overall mechanical properties, the NP's effect will be increased (at a given loading and assuming random dispersion) when either the interfacial properties are more different than the bulk or the interfacial effects persist to longer range (as each NP will impact more material).[62,63] We only coarsely resolved the distance to which the bond dynamics were impacted, as the statistics are poor when considering small shells around the polymer. Specifically, we find the first shell is significantly impacted and the properties of the second shell (beyond 2σ) are close to those of the bulk for all systems. Note that we do see some differences in the location of the peak in g(r) relating to ion packing around the NP, as discussed above. Considering the degree to which the ionomer is impacted within 2σ from the interface, ion content clearly has a significant effect. We can

see this by comparing lowest (N_{bb}3-10%Na) and highest (N_{bb}-75%Na) ion content systems studied. Specifically, at the lowest ion content of 4% (percentage of charged beads to total beads) and for sticky NPs that have the larger effect on the surrounding ionomer, the interfacial bond relaxation time (where the BACF crosses 1/e) is 46% faster than in bulk. Meanwhile, at the highest ion content of 33%, bond relaxation time is more than 10 times slower than in the bulk, a much larger relative change. The overall mechanical properties of a nanocomposite at high loading will also depend on whether the interfacial regions overlap.

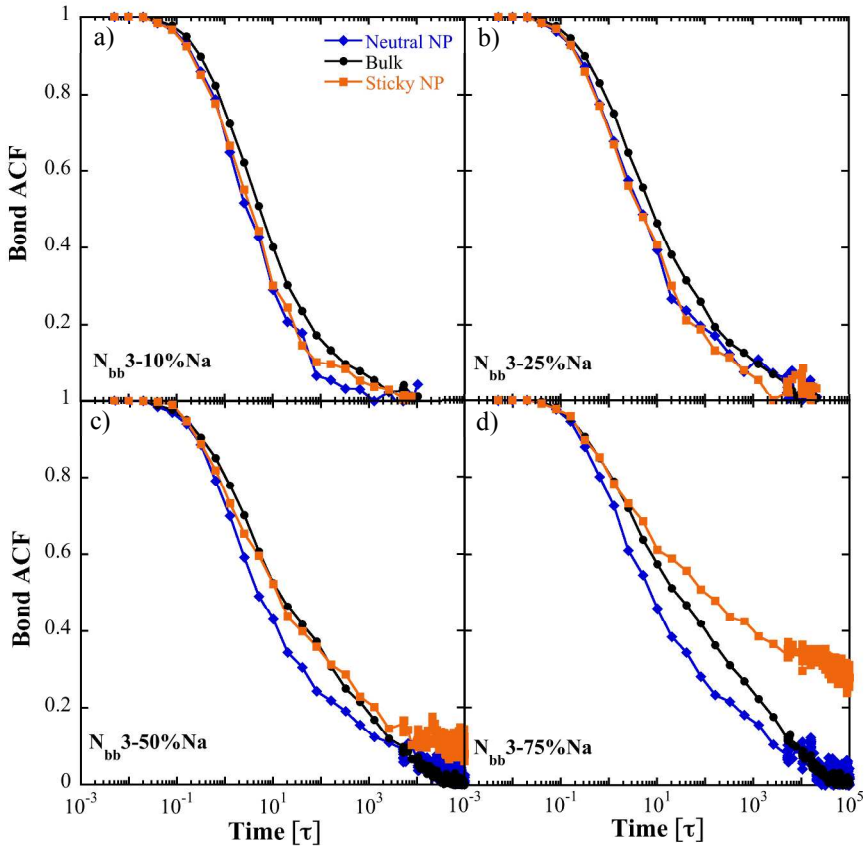

Figure 8: Bond vector autocorrelation function for bonds near the surface of a neutral or sticky NP or in bulk, as labeled, for (a) N_{bb}3-10%Na, (b) N_{bb}3-25%Na, (c) N_{bb}3-50%Na, and (d) N_{bb}3-75%Na.

Finally, we analyze the effect of NP size (curvature) on the structure and dynamics of the ionomer by considering systems with NPs of diameters 7.5σ and 12.5σ (and compare the results to those of 10σ particles discussed above). We add a larger amount of polymer around the larger particles to keep the same low loading fraction. Figure 9 shows the pair correlation functions for the N_{bb}5-50%Na systems for the different NP sizes. The distribution of different moieties around the neutral NP is very similar across the systems, implying that the relatively modest change in curvature of the NP over this diameter range doesn't significantly affect the packing around the neutral NP. For the case of the sticky NP, the first NP-ion peak is highest when the NP diameter is 7.5σ, with an intensity of 27, then remains similar at 18.5 for the two higher NP diameters; this reflects a slightly greater ordering of ions at the smaller sticky NP's surface. The later peaks are similar for systems with different sizes of sticky NPs. The BACF was also calculated for the three systems with different NP diameters as a function of distance from the NP (see Figure 10). We observe the same trend as discussed above—the bonds near the sticky NP interface relax slower than the bulk, whereas those near the neutral NP interface relax faster. This trend is consistent across the systems, and does not change with NP size. Overall, changing the NP size within this range does not significantly affect the distribution of ions or their dynamics around the NP.

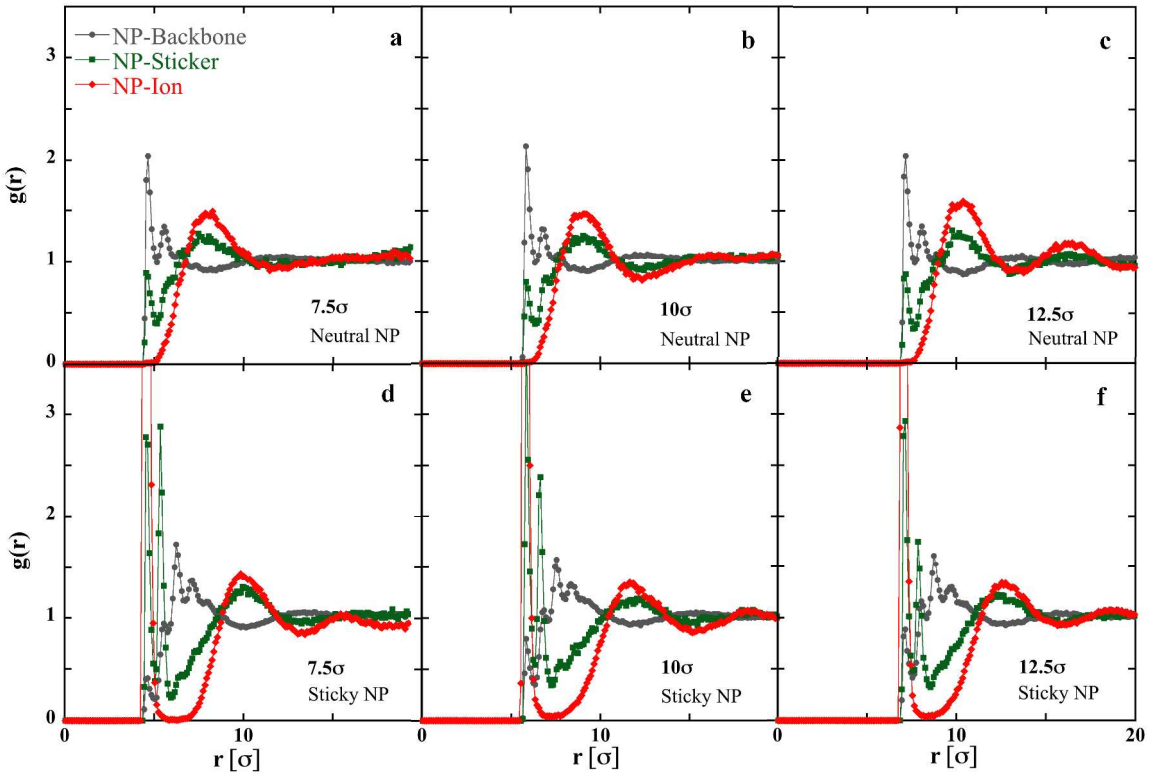

Figure 9: NP-Backbone, NP-Sticker, and NP-Ion pair correlation functions for three N_{bb}5-50%Na systems with NP diameters of 7.5σ (a,d), 10σ (b,e), and 12.5σ (c,f); a-c (top row) are for a neutral NP and d-f (bottom row) are for a sticky NP.

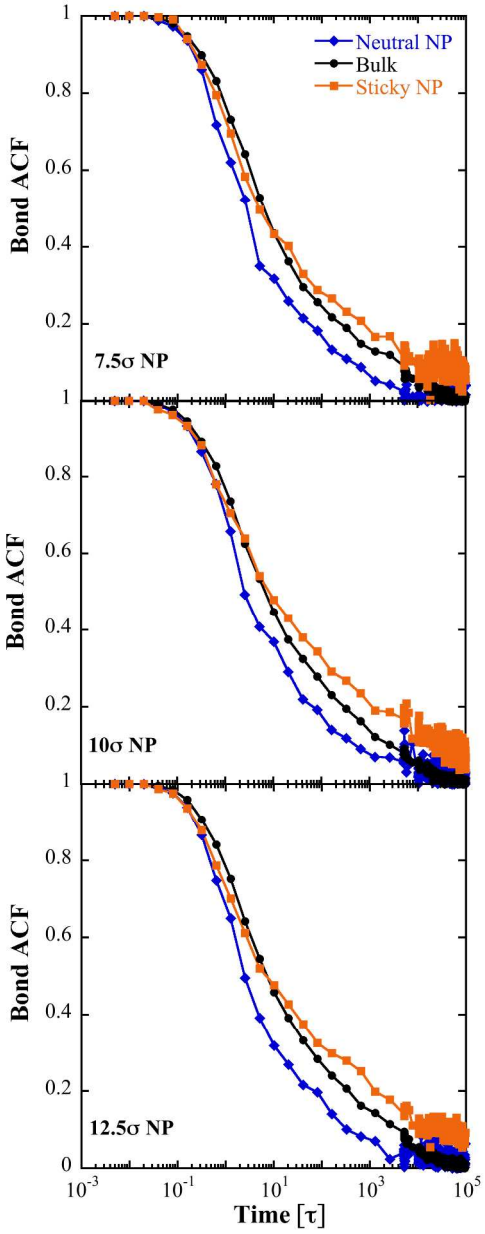

Figure 10: Bond vector autocorrelation function near the surface of the NP and in the bulk for sticky and neutral NP systems, for three systems with different NP sizes, as labeled.

Conclusions:

We used MD to study the behavior of ionomer melts as a function of distance from an added NP, with varying ionomer spacer length and neutralization level. We considered

either a weakly attractive (neutral) NP or an NP that is strongly attractive (sticky) with respect to associating polymer groups, and we compare how the different ionomer structures and ion-NP interactions impact aggregate structure and dynamics. Ions are depleted around a neutral NP versus the bulk, for a distance of about 2-3σ from the surface. In contrast, the ions and stickers are well ordered and present at increased density near the surface of a sticky NP. By comparing the position of the first NP-ion peak in the radial distribution function, it is seen that the aggregates move closer to the NP when the ion density is high (when average spacing between ions on polymer chains is shorter or when ion neutralization level is higher). To study the effect of NP size, we simulated an intermediate type of ionomer with NPs of diameters 7.5σ, 10σ, and 12.5σ, maintaining a constant low NP loading such that polymer reaches bulk properties by the edge of the simulation box. We conclude that there is no major change in the interfacial behavior as a function of NP size in this range.

To understand the effect of the structural inhomogeneity brought about by the NP on the dynamics of the system, we calculated the bond autocorrelation function in radial shells around each NP. Bond vector relaxation around the interface of the neutral NP is faster than in the bulk, while bond dynamics are slowed around the sticky NP (for high ion density systems, the bonds around the sticky NP do not completely decorrelate even over the longest time analyzed). It is seen that for systems at the same neutralization, the bond dynamics are more impacted near the interface for systems that have higher spacer length. For systems at low neutralizations of 10% and 25% (which contain more stickers than ions), the interfacial bond dynamics for both neutral and sticky NPs are relatively

similar. Overall, increasing neutralization or increasing spacer length increases the impact that NPs have on the interfacial behavior in these ionomer nanocomposites.

Broadly, we find that NP-ion interactions are crucial in determining ionic aggregate structure and dynamics near the interface. We considered only a single isolated NP in the current work. However, an interesting question for future work would be to study NP-NP interactions as a function of ion content and NP-monomer interaction strength, as we expect that the interfacial structural changes observed here likely also have a strong impact on overall NP dispersion.

Conflicts of interest:

There are no conflicts to declare

Acknowledgements:

We thank Jonathan Brown for providing the cluster analysis script, and Connor H. Barber for his help in modifying parts of this script. This work was supported in part by the National Science Foundation, under Grant 1463103. This work was also supported by an allocation in computing time from the Ohio Supercomputer Center.

References:

1 J. Njuguna and K. Pielichowski, *Adv. Eng. Mater.*, 2003, **5**, 769–778.

2 H. Xu, L. Cheng, C. Wang, X. Ma, Y. Li and Z. Liu, *Biomaterials*, 2011, **32**, 9364–9373.

3 J. Liu, L. Zhang, D. Cao and W. Wang, *Phys. Chem. Chem. Phys.*, 2009, **11**, 11365.

4 V. Ganesan and A. Jayaraman, *Soft Matter*, 2014, **10**, 13–38.

5 X. Zheng, M. H. Rafailovich, J. Sokolov, Y. Strzhemechny, S. . Shwarz, B. . Sauer and M. Rubinstein, *Phys. Rev. Lett.*, 1997, **79**, 241–244.

6 J. A. Forrest, K. Dalnoki-Veress, J. R. Stevens and J. R. Dutcher, *Phys. Rev. Lett.*, 1996, **77**, 2002–2005.

7 F. W. Starr, T. B. Schrøder and S. C. Glotzer, *Macromolecules*, 2002, **35**, 4481–4492.

8 J. T. Kalathi, S. K. Kumar, M. Rubinstein and G. S. Grest, *Soft Matter*, 2015, **11**, 4123.

9 R. L. Jones, S. K. Kumar, D. L. Ho, R. M. Briber and T. P. Russell, *Nature*, 1999, **400**, 146–149.

10 G. Fleer, M. . Cohen Stuart, J. M. H. . Scheutjens, T. Cosgrove and B. Vincent, *Polymers at Interfaces*, Chapman and Hall, London, 1993.

11 M. R. Tant, K. A. Mauritz and G. L. Wilkes, *Ionomers: synthesis,structure,properties and application*, Blackie Academic & Professional, 1997.

12 J. A. Lee, M. Kontopoulou and J. S. Parent, *Polymer (Guildf).*, 2005, **46**, 5040–

5049.

13 S. D. Benson and R. B. Moore, *Polymer (Guildf).*, 2010, **51**, 5462–5472.

14 M. E. Seitz, C. D. Chan, K. L. Opper, T. W. Baughman, K. B. Wagener and K. I. Winey, *J. Am. Chem. Soc.*, 2010, **132**, 8165–8174.

15 P. Vanhoorne and R. A. Register, *Macromolecules*, 1996, **29**, 598–604.

16 N. K. Tierney and R. A. Register, *Macromolecules*, 2002, **35**, 6284–6290.

17 J. Sampath and L. M. Hall, *Macromolecules*, 2018, **51**, 626–637.

18 L. R. Middleton and K. I. Winey, *Annu. Rev. Chem. Biomol. Eng.*, 2017, **8**, 22.1-22.25.

19 L. R. Middleton, S. Szewczyk, J. Azoulay, D. Murtagh, G. Rojas, K. B. Wagener, J. Cordaro and K. I. Winey, *Macromolecules*, 2015, **48**, 3713–3724.

20 E. B. Trigg, M. J. Stevens and K. I. Winey, *J. Am. Chem. Soc.*, 2017, **139**, 3747–3755.

21 D. S. Bolintineanu, M. J. Stevens and A. L. Frischknecht, *Macromolecules*, 2013, **46**, 5381–5392.

22 D. S. Bolintineanu, M. J. Stevens and A. L. Frischknecht, *ACS Macro Lett.*, 2013, **2**, 206–210.

23 C. L. Ting, M. J. Stevens and A. L. Frischknecht, *Macromolecules*, 2015, **48**, 809–818.

24 C. L. Ting, K. E. Sorensen-Unruh, M. J. Stevens and A. L. Frischknecht, *J. Chem. Phys.*, 2016, **145**, 44902.

25 L. M. Hall, M. E. Seitz, K. I. Winey, K. L. Opper, K. B. Wagener, M. J. Stevens and A. L. Frischknecht, *J. Am. Chem. Soc.*, 2012, **134**, 574–587.

26 L. M. Hall, M. J. Stevens and A. L. Frischknecht, *Phys. Rev. Lett.*, 2011, **106**, 127801.

27 L. M. Hall, M. J. Stevens and A. L. Frischknecht, *Macromolecules*, 2012, **45**, 8097–8108.

28 J. Sampath and L. M. Hall, *J. Chem. Phys.*, 2017, **147**, 134901.

29 C. Wong and J. H. R. Clarke, *J. Chem. Phys.*, 2002, **116**, 6795–6802.

30 M. Goswami, S. K. Kumar, A. Bhattacharya and J. F. Douglas, *Macromolecules*, 2007, **40**, 4113–4118.

31 E. Allahyarov and P. L. Taylor, *J. Chem. Phys.*, 2007, **127**, 154901.

32 D. J. Yarusso and S. L. Cooper, *Macromolecules*, 1983, **16**, 1871–1880.

33 D. J. Kinning and E. L. Thomas, *Macromolecules*, 1984, **17**, 1712–1718.

34 J. H. Jang, R. Ozisik and W. L. Mattice, *Macromolecules*, 2000, **33**, 7663–7671.

35 C. Ayyagari, D. Bedrov and G. D. Smith, *Polymer (Guildf).*, 2004, **45**, 4549–4558.

36 B. B. Sauer and R. S. McLean, *Macromolecules*, 2000, **33**, 7939–7949.

37 A. Bansal, H. Yang, C. Li, K. Cho, B. C. Benicewicz, S. K. Kumar and L. S. Schadler, *Nat. Mater.*, 2005, **4**, 693–698.

38 F. W. Starr, T. B. Schrøder and S. C. Glotzer, *Phys. Rev. E*, 2001, **64**, 21802.

39 D. Ruan and D. S. Simmons, *Macromolecules*, 2015, **48**, 2313–2323.

40 D. Ruan and D. S. Simmons, *J. Polym. Sci. Part B Polym. Phys.*, 2015, **53**, 1458–1469.

41 F. W. Starr, J. F. Douglas and S. C. Glotzer, *J. Chem. Phys.*, 2003, **119**, 1777–1788.

42 G. D. Smith, D. Bedrov, L. Li and O. Byutner, *J. Chem. Phys.*, 2002, **117**, 9478–

9490.

43 A. Karatrantos, N. Clarke, R. J. Composto and K. I. Winey, *Soft Matter*, 2016, **12**, 2567–2574.

44 A. Karatrantos, N. Clarke, R. J. Composto and K. I. Winey, *Soft Matter*, 2015, **11**, 382–388.

45 J. Liu, Y. Wu, J. Shen, Y. Gao, L. Zhang and D. Cao, *Phys. Chem. Chem. Phys.*, 2011, **13**, 13058.

46 G. J. Papakonstantopoulos, M. Doxastakis, P. F. Nealey, J. L. Barrat and J. J. De Pablo, *Phys. Rev. E - Stat. Nonlinear, Soft Matter Phys.*, 2007, **75**, 1–13.

47 P. J. In'T Veld, M. A. Horsch, J. B. Lechman and G. S. Grest, *J. Chem. Phys.*, 2008, **129**, 164504.

48 G. S. Grest, Q. Wang, P. I. T. Veld and D. J. Keffer, *J. Chem. Phys.*, 2011, **134**, 144902.

49 Y. Li, M. Kröger and W. K. Liu, *Soft Matter*, 2014, **10**, 1723.

50 V. Pryamitsyn and V. Ganesan, *Macromolecules*, 2006, **39**, 844–856.

51 S. Sen, J. D. Thomin, S. K. Kumar and P. Keblinski, *Macromolecules*, 2007, **40**, 4059–4067.

52 A. Ghanbari, M. Rahimi and J. Dehghany, *J. Phys. Chem. C*, 2013, **117**, 25069–25076.

53 K. Kremer and G. S. Grest, *J. Chem. Phys.*, 1990, **92**, 5057.

54 J. T. Kalathi, G. S. Grest and S. K. Kumar, *Phys. Rev. Lett.*, 2012, **109**, 1–5.

55 M. E. Mackay, A. Tuteja, P. M. Duxbury, C. J. Hawker, B. Van Horn, Z. Guan, G. Chen and R. S. Krishnan, *Science (80-.).*, 2006, **311**, 1740–1743.

56 S. Plimpton, *J. Comput. Phys.*, 1995, 117, 1–19.

57 S. J. Plimpton, R. Pollock and M. J. Stevens, in *Proceedings of the Eighth SIAM Conference on Parallel Processing for Scientific Computing*, Minneapolis, 1997.

58 W. Humphery, A. Dalke and K. Schlten, *J. Molec. Graph.*, 1996, **14**, 33–38.

59 G. . Schneider, K. Nusser, L. Willner, P. Falus and D. Richter, 2011, **44**, 5857–5860.

60 J. V. Heffernan, J. Budzien, F. Avila, T. C. Dotson, V. J. Aston, J. D. McCoy and D. B. Adolf, *J. Chem. Phys.*, 2007, **127**, 214902.

61 A. M. Castagna, W. Wang, K. I. Winey and J. Runt, *Macromolecules*, 2011, **44**, 5420–5426.

62 P. J. Griffin, V. Bocharova, L. R. Middleton, R. J. Composto, N. Clarke, K. S. Schweizer and K. I. Winey, *ACS Macro Lett.*, 2016, **5**, 1141–1145.

63 N. Jouault, M. K. Crawford, C. Chi, R. J. Smalley, B. Wood, J. Jestin, Y. B. Melnichenko, L. He, W. E. Guise and S. K. Kumar, *ACS Macro Lett.*, 2016, **5**, 523–527.

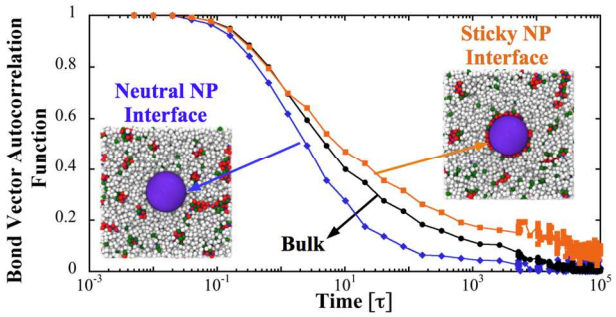

Ions are depleted around a neutral nanoparticle and denser around a sticky nanoparticle, impacting bulk vs. interfacial ionomer dynamics